

ANALYSIS OF Ta-RICH MX PRECIPITATES IN RAFS—H. Tanigawa (Japan Atomic Energy Research Institute), H. Sakasegawa (Kyoto University), N. Hashimoto, S. J. Zinkle, and R. L. Klueh (Oak Ridge National Laboratory), and A. Kohyama (Kyoto University)

OBJECTIVE

The objective of this work is to analyze the precipitate distribution with emphasis on Ta-rich MX precipitate in reduced-activation ferritic/martensitic steels (RAFs) by observing the extraction replica samples with TEM and SEM.

SUMMARY

Extraction replica samples were prepared from F82H-IEA, F82H HT2, JLF-1 and ORNL9Cr to analyze the precipitate distribution. The samples were examined to obtain precipitate size distribution with TEM and to analyze chemical composition distribution with SEM. Back-scattered electron imaging was found to be the effective way to separate Ta-rich precipitate from other precipitates. Results showed that most of the precipitates were $M_{23}C_6$, and the shape is a round ellipsoid in F82H-IEA and HT2, but was a long ellipsoid in JLF-1 and ORNL9Cr. It was also found that MX precipitates were few and large and contain Ti in F82H-IEA and HT2, but a lot of fine MX precipitates without Ti were observed in JLF-1 and ORNL9Cr.

PROGRESS AND STATUS

Introduction

Using extraction replica samples for precipitate analysis is the typical method for the investigation of precipitation in irradiated steels. The critical point of this method is the fact that the area to be analyzed for its chemical composition tends to be limited to a few tenths of a micron (generally less than $10\mu m$) square. This limitation makes it difficult to find minor precipitates such as MX, and it also makes it difficult to increase the statistical accuracy. In this study, FE-SEM and TEM were used for the observation of replica samples to analyze a wider region. A new technique to detect Ta-rich precipitates was proposed.

Experimental

Materials used in these experiments are IEA-modified F82H (F82H-IEA), another heat treatment of F82H (F82H HT2), ORNL9Cr-2WVTa (ORNL9Cr) and JLF-1 HFIR heat (JLF-1). The details of these steels were shown in another paper [1]. Extraction replicas were made from the cross section of 1/3CVN specimens. The specimen surface was first mechanically polished and then electropolished with 8% sulfuric acid, 1% hydrofluoric acid, and methanol before etching. Then the surface was electroetched with 10% hydrochloric acid in methanol and carbon coated to make the replica. The replica was removed by weak electroetching and collected in dilute ethanol on a mesh.

TEM (JEOL 2000FX) and FE-SEM (Philips XL30FEG) was used for the analyses of replica samples. FE-SEM operated at 15kV was used for observation with a secondary electron (SE) imaging mode and with a back-scattered electron (BSE) imaging mode, and it was used for chemical analysis with X-ray energy-dispersive spectrometry (XEDS) system. The XEDS mapping was done for $10\mu m$ square areas with a resolution of 80 nm and 3.0 s dwell time per spot.

Results and Discussion

Fig. 1 shows the typical TEM images of replica samples of each RAFs around a triple point of a prior austenitic grain. It shows that; (1) number density of precipitates in JLF-1 and ORNL9Cr is larger than that of in F82H-IEA and F82H HT2, (2) precipitates in JLF-1 are larger than those of other RAFs, and (3) precipitates in JLF-1 and ORNL9Cr had relatively longer ellipsoid shape compared to those of F82H-IEA and F82H HT2. The tendency suggested in (1) and (2) coincides with the results obtained from extraction residue samples [2].

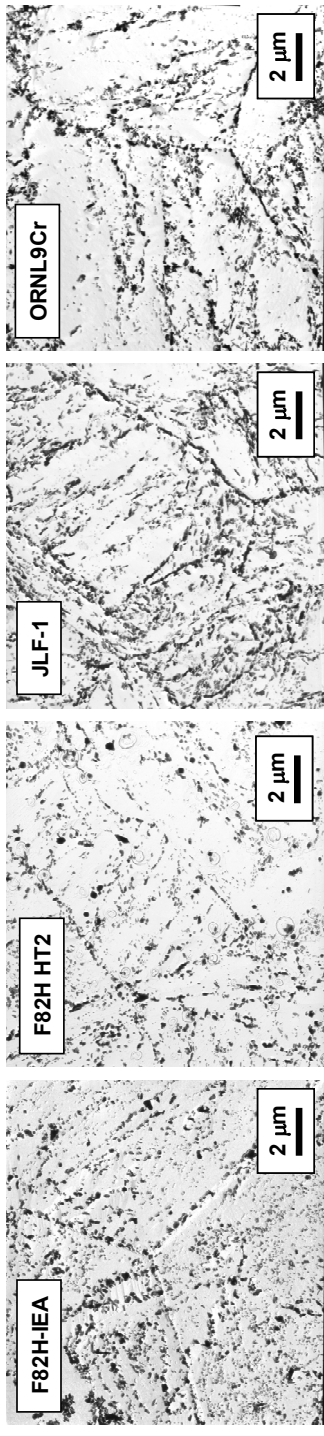


Fig. 1. TEM bright field images of replica samples made from each RAFs.

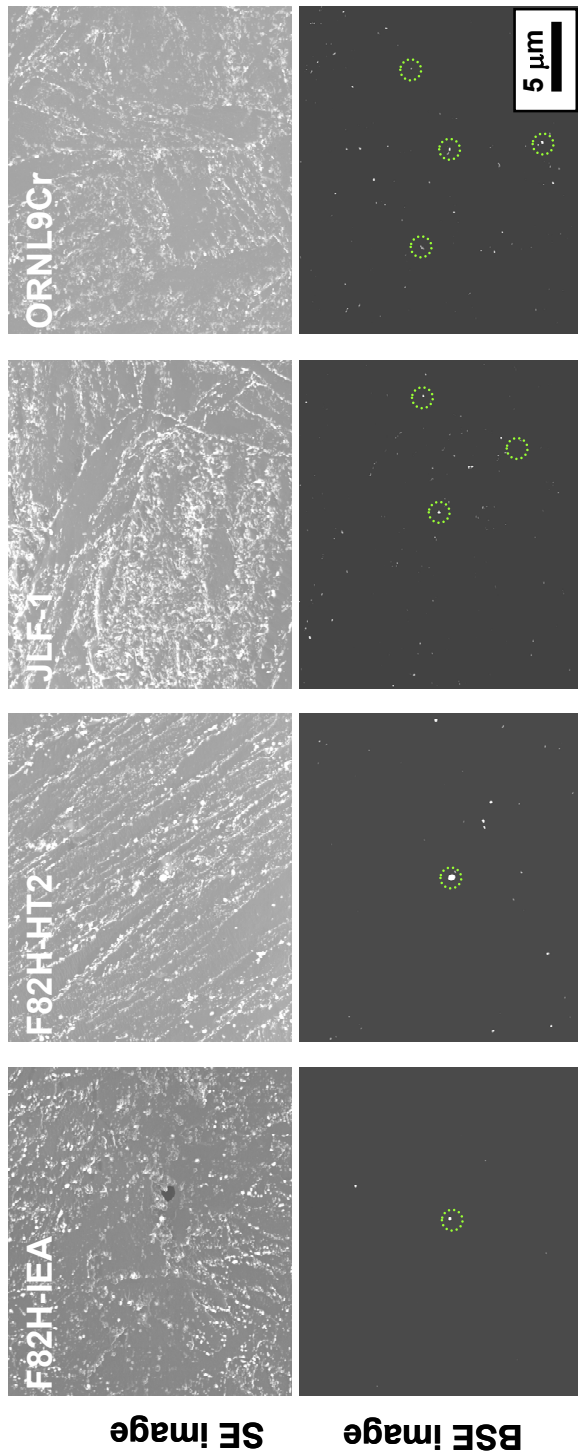


Fig. 2. Secondary electron (SE) and back-scattered electron (BSE) images of replica samples made from each RAFs. Green dotted circles in BSE images indicate the MX precipitates.

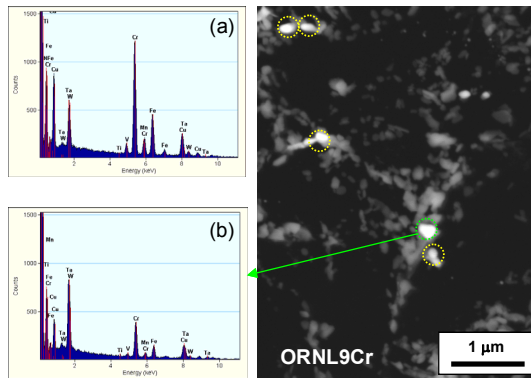


Fig. 3. High contrast BSE images of replica sample from ORNL9Cr. (a) shows EDS peaks from dark contrast precipitates or bright precipitates encircled by a dotted yellow line, and (b) shows the peaks from bright precipitate encircled by a dotted green line.

Fig. 2 shows the SE and BSE images of replica samples of each RAFs. The BSE image with high contrast condition gave a bright image of some precipitates. EDS mapping suggested that most of the precipitates are Cr rich, i.e., $M_{23}C_6$ (M; Cr, W, Fe) precipitates. XEDS analyses on each of those bright imaged precipitates revealed that some of the precipitates contain tantalum, i.e., MX (M;Ta,V,Ti :X ; C, N) precipitates, and others are large or double-layered $M_{23}C_6$ precipitates (Fig. 3). This is similar to Z-contrast images usually obtained by HAADF (high-angle annular dark field) imaging in STEM. Fig. 4 shows the number density and average size of MX precipitates (white arrows in Fig. 2). The result suggests that large, spherical-shaped and a low number density of MX precipitates were observed in F82H-IEA and F82H HT2, but small and a relatively high number density of MX precipitates were observed in JLF-1 and ORNL9Cr. A high density of MX precipitates in JLF-1 and ORNL9Cr is quite reasonable as those steels have higher Ta (0.07 and 0.09 wt%, respectively) compared to that of F82H (0.02wt%). It should be noted that all MX precipitates in F82H contain Ti. This is also reasonable as F82H contains a relatively higher Ti (0.01wt%) compared to the other RAFs. It is known that Ti forms $Ti(C,N)$ that is stable at high temperature ($\sim 1473K$), and $Ti(C,N)$ could become the nucleus of MX precipitates [3]. Therefore, it could be concluded that Ti ($Ti(C,N)$) contributed to the formation and stabilization of large MX precipitates in F82H.

It should be noted that about 1/3 of the MX precipitates in ORNL9Cr were accompanied by Mo- and Mn-rich precipitates. Fig. 5 shows how the

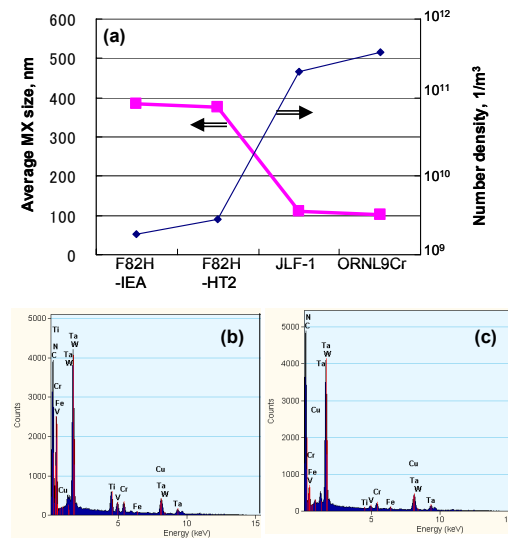


Fig. 4. (a) Number density and average size of MX (TaC) precipitates of each RAFs, (b) typical EDX peaks obtained from MX precipitates in F82H-IEA and F82H HT2, and (c) those from JLF-1 and ORNL9Cr.

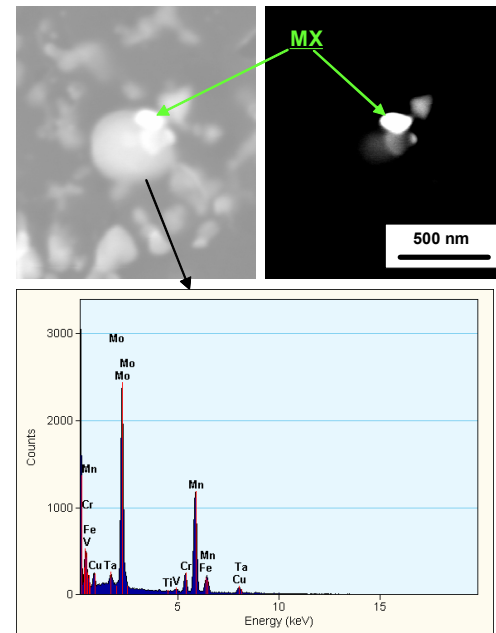


Fig. 5. Mo- and Mn-rich precipitate observed next to MX precipitates in ORNL9Cr.

large (~400nm diameter) and spherical-shaped Mo/Mn-rich precipitates were usually located just below the MX precipitates. This type of precipitate is not expected, as Mo and Mn are generally believed to be included in $M_{23}C_6$ or in the matrix as solute, and it has not been reported to form this type of precipitate. Further analyses on this will be conducted in the future.

SUMMARY AND CONCLUSIONS

Extraction replica samples were prepared from F82H-IEA, F82H HT2, JLF-1 and ORNL9Cr to analyze the precipitate distribution. The samples were examined to obtain precipitate size distribution with TEM, and to analyze chemical composition distribution with SEM. The following is a summary of the important observations and conclusions:

- (1) Results show that most of the precipitates are $M_{23}C_6$ with a round ellipsoid shape in F82H-IEA and HT2, but with a long ellipsoid shape in JLF-1 and ORNL9Cr.
- (2) Back-scattered electron imaging was found to be the effective way to separate Ta-rich precipitate from other precipitates.
- (3) MX precipitates were few and large and contain Ti in F82H-IEA and HT2, but a lot of fine MX precipitates without Ti were observed in JLF-1 and ORNL9Cr.
- (4) About 1/3 of MX precipitates in ORNL9Cr were found to be accompanied by large and spherical-shaped Mo/Mn-rich precipitates.

Acknowledgements

The authors would like to thank Mr. J.L. Bailey and J.W. Jones for their help on preparing specimens for this experiment. This research was sponsored by the Japan Atomic Energy Research Institute and the Office of Fusion Energy Sciences, US Department of Energy under contract DE-AC05-00OR22725 with UT-Battelle.

References

- [1] H. Tanigawa, M. A. Sokolov, K. Shiba, and R. L. Klueh, *Fusion Sci. Tech.* 44 (2003) 206.
- [2] H. Tanigawa, H. Sakasegawa, S. J. Zinkle, R. L. Klueh, and A. Kohyama, in this semiannual report.
- [3] M. Tamura, K. Shinozuka, K. Masamura, K. Ishikawa, and S. Sugimoto, 258-263 (1998) 1158.